Use of Polyurethane Precursor-Based Modifier as an Eco-Friendly Approach to Improve Performance of Asphalt

Tianshuai Li[1]; Nicolás Héctor Carreño Gómez[2]; Guoyang Lu, Ph.D.[3]; Dong Liang, Ph.D.[4]; Dawei Wang, Ph.D.[5]; and Markus Oeser, Ph.D.[6]

1. *Ph. D candidate, School of Transportation Science and Engineering, Harbin Institute of Technology, 73 Huanghe Rd., Nangang District, Harbin 150090, P.R.China. Email: 17B932006@stu.hit.edu.cn;*
2. *Ph. D candidate, Institute of Highway Engineering, RWTH Aachen University, Mies-van-der-Rohe-Street 1, 52074 Aachen, Germany. Email: carreno@isac.rwth-aachen.de;*
3. *Ph. D, Civil and Environmental Engineering, The Hong Kong Polytechnic University, 11 Yuk Choi Road, Hung Hom, Kowloon, Hong Kong. Email: lu@isac.rwth-aachen.de;*
4. *Ph. D, BASF Polyurethane Specialties (China) Company Ltd., JiangXinSha Road, PuDong New District, Shanghai 200137, P.R.China. Email: dong.liang@basf.com*
5. *Ph. D, Professor, School of Transportation Science and Engineering, Harbin Institute of Technology, 73 Huanghe Rd., Nangang District, Harbin 150090, P.R.China; Professor, Institute of Highway Engineering, RWTH Aachen University, Mies-van-der-Rohe-Street 1, 52074 Aachen, Germany (corresponding author). Email: wang@isac.rwth-aachen.de;*
6. *Ph. D, professor, Institute of Highway Engineering, RWTH Aachen University, Mies-van-der-Rohe-Street 1, 52074 Aachen, Germany; Professor, School of Transportation Science and Engineering, Harbin Institute of Technology, 73 Huanghe Rd., Nangang District, Harbin 150090, P.R.China. Email: oeser@isac.rwth-aachen.de;*

**Corresponding Author: Dawei WANG, Prof. Dr.-Ing., School of Transportation Science and Engineering, Harbin Institute of Technology, 73 Huanghe Rd., Nangang District, Harbin 150090, China; Professor, Institute of Highway Engineering, RWTH Aachen University, Mies-van-der-Rohe-Street 1, 52074 Aachen, Germany. Tel: +49-241-8026742, Fax: +49-241-8022141; Email: wang@isac.rwth-aachen.de*

Abstract

With the rapid growth of traffic demands, using liquid chemical material instead of traditional modifier to prepare high-performance modified asphalt demonstrates dual values in environmental protection and performance improvement of pavement. The objective of this study is to assess the efficiency and reveal the modification mechanism of using a developed polyurethane-precursor based reactive modifier (PRM) in the preparation of polyurethane-precursor modified asphalt (PMA). The selected petroleum asphalts (60/80 pen grade) were modified at 1.5%, 2.5% and 4% by weight. Samples of the base asphalt and PMA binders were characterized by Dynamic Shear Rheometer (DSR), Time Sweep (TS) fatigue test and Single Edge Notched Beam (SENB) tests. The modification mechanism was finally demonstrated by the fraction analysis, Fourier-transform Infrared Spectroscopy (FTIR), Differential Scanning Calorimeter (DSC), Atomic Force Microscopy (AFM), Fluorescence Microscope (FM). Due to the presence of polar groups in neat asphalt, the usage of PRM can be treated as a chemical method for the modification and it shows good compatibility with neat asphalt. The incorporation of PRM to the asphalt matrix can remarkably improve the high-temperature performance and fatigue resistance of asphalt. Besides, the PMA presents desirable low-temperature crack resistance and aging resistance. Considering the relatively low level of preparation temperature (145°C) and the huge improvement in high-temperature performance, the modification using PRM can be regarded as an environmentally friendly alternative for the production of polymer modified asphalt, especially at high-temperature regions.

Keywords: polyurethane-precursor-based reactive modifier; modified asphalt; pavement performance; modification mechanism

Introduction

Asphalt mixture is a typical multi-phase heterogeneous material that includes air-voids, aggregates and asphalt binder (Shi et al. 2014; Lv et al. 2018). As the binding agent of aggregate, asphalt plays an important role in the mechanical and functional performance of the asphalt pavement (Zhang et al. 2010). However, with the rapid growth of traffic demands, the neat or the modified asphalt binders cannot show promising engineering performances under some conditions. This has led to an urgent requirement to improve the performance of existing asphalt binders. Polymers such as styrene-butadiene-styrene (SBS) (Yin et al. 2017; Lu et al. 1998), styrene-butadiene rubber (SBR) (Shadmani et al. 2018; Khabaz et al. 2015), ethylene-vinyl acetate (EVA) (Liang et al. 2017; Yuliestyan et al. 2016; Airey et al. 2002), crumb rubber (CR) (Yang et al. 2017; Presti et al. 2013; Singh et al. 2020), have been extensively incorporated into neat asphalt as the modification additives to mitigate the pavement failures (Xiao et al. 2014; Wekumbura et al. 2007; Ali et al. 2014). Although the polymer modification can generally improve the performance of asphalt, there are still some aspects that need to be cared for. For instance, the layered segregation of modified asphalt can easily occur during storage at high temperatures. The blending and swelling of polymers in asphalt need high production temperatures, which consumes more energy. Besides, the potential greenhouse gas emissions and related air pollution from the asphalt binder and polymer itself at high temperatures have not been well treated (Yang et al. 2017; Li et al. 2016; Ji et al. 2020).

Polyurethane is a compound containing urethane groups (-NHCOO-) in molecule chains stemming from the reaction of isocyanate-based materials (contain -NCO functional groups) with polyols (contain -OH groups) (Lu et al. 2019;). Polyurethane-precursors containing isocyanate functionalities can easily react with various

compounds containing functional groups such as hydroxyl groups or amino groups. The most common reaction occurred between isocyanates and hydroxyl groups (Mondal et al. 2004) is:

$$\text{R-NCO} + \text{R'-OH} \rightarrow \text{R-NH-CO-O-R'}$$

Thanks to the wide presence of free radicals (such as –OH, –NH, -NH2) in asphalt binders, a polyurethane-precursor-based reactive modifier and asphalt have a certain natural affinity and chemical basis for modification.

Due to the PRM used for the studies presented herein being a liquid modifier, it is not necessary to use the colloidal mill to grind the solid polymer modifier at the preparation of modified asphalt. Thus, the production process can be simplified, and the equipment cost can be reduced. The liquid-liquid blending is much easier than liquid-solid blending and the production temperature is expected to be reduced to 140-150°C, which leads to lower energy consumption. Besides, the decrease in production temperature can also effectively reduce the damage of neat asphalt caused by high temperatures. Overall, the production of modified asphalt using PRM provides unique advantages in the simplification of the production process, improvement of blending efficiency, and reduction of production temperature. It is an ideal, ecological, and economically viable material for asphalt modification.

In recent years, reactive modification has become a prevalent research objective gaining sustained attention. The suitability of polyurethane-precursor-based/ polyurethane-based materials as a reactive modifier to prepare modified asphalt has been investigated. Singh et al. (2003) evaluated the effect of isocyanate production waste particles on the thermal and rheological properties of waterproofing bitumen. Fang et al. (2016) characterized an isocyanate and nanoparticles composite modified asphalt by taking physical tests, SEM, fluorescence microscopy and FTIR tests. Carrera andMartín-

Alfonso et al. (2009, 2010) studied the polyurethane-precursor-based modification on the neat asphalt using an isocyanate-based reactive polymer (MDI-PPG) that is synthesized by reacting MDI (4,4' -diphenylmethane diisocyanate) with polyethylene-glycol (PPG). Yu et al. (2017) used a nano polyurethane emulsion (WPU) as a polymer modifier to prepare modified asphalt. Using the renewable castor oil and liquefied MDI, the castor oil-polyurethane prepolymer (C-PU) terminated with the NCO group was synthesized as an asphalt modifier and C-PU modified asphalt with 10-40 % C-PU were prepared by Xia et al. (2016). According to the results of the mechanical and microscopic investigations of the above studies, the modifications delivered both good pavement properties and well-developed polymeric networks. Besides, as an important form of chemical modification, the previous research of polyphosphate acid (PPA) modified asphalt can also provide a reference for this study. It was generally accepted that the active groups in asphalt can react with PPA through salt-forming and esterification reactions, which lead to the change in the physicochemical state of asphalt binders (Baumgardner et al. 2005; Liu et al. 2018; Mousavi et al. 2019).

Although the rheological and chemical performance of modified asphalts involving polyurethane-precursor-based/ polyurethane-based modifiers has been reported in some previous studies, the preparation of such modifiers for accurately controlling the performance of accordingly modified asphalt products is challenging. Therefore, it is pertinent to propose a suitable reactive modifier and understand the mechanical-chemical properties of modified asphalt binders from the perspective of laboratory tests. This can not only further clarify the technical performance and modification mechanism but also lay the foundation for the large-scale application in the paving trials. Besides, the potential values of PRM modified asphalt in energy conservation and environmental protection can be further developed.

The objective of this research is to evaluate the pavement performance and modification mechanism of a novel polyurethane-precursor-based reactive modifier for asphalt binders (PRM) which features isocyanate functional groups. Based on the selected type of PRM, the modified asphalt binders were prepared by means of laboratory mixing. The comprehensive performance and modification mechanism were further studied.

Experimental programs

Materials

In this research, the base (neat) asphalts (DS 70#) having 60/80 penetration grade produced by Desheng Haoye Chemical Industry, Liaoning, China were used. The main physical properties of the neat asphalt were determined according to JTG F40-2004 and are shown in **Table 1**.

The polyurethane-precursor-based reactive modifier containing isocyanate functional groups (PRM) was obtained and employed to prepare PRM modified asphalt binders (marked as PMA).

Sample preparation

The modified asphalts were prepared using a high shear mixer (HSM-100L) manufactured by ROSS Equipment Co. Ltd. 850 g of neat asphalt was poured into a metal container, then it was heated up to the blending temperature of 145°C. During this period, the shear speed was set as 300 r/min. The PRM has added to the asphalt within 20 minutes afterwards and then sheared at the shearing speed of 3000 r/min for more than 80 minutes. In this research, The PMAs with 1.5%, 2.5% and 4% (by weight of base asphalt) PRM were marked as DS+1.5%, DS+2.5% and DS+4%, respectively.

151 ***Test methods***

152 **Dynamic Shear Rheometer (DSR) test**

153 The rheological behaviors of the neat asphalt and polyurethane modified asphalts were
154 measured by the ARES-G2 rotational rheometer made by TA Instruments, USA. The
155 complex shear modulus (G*) and the phase angle (°) were obtained within the scope of
156 linear viscoelastic (LVE). Frequency sweeps were carried out over a range of 0.1- 30
157 Hz at a series of specified temperatures (0, 12, 24, 36, 48, 60, 72 and 84°C). The results
158 of the G* and δ obtained from the frequency sweep test were then used for the
159 construction of master curves at the reference temperature based on the WLF equation.
160 In this study, the reference temperature is chosen at an intermediate temperature of
161 36 °C. The mater curve established at this temperature can be used to effectively
162 illustrate the properties of asphalt under high and low loading frequencies. The rutting
163 parameter of G*/sinδ (at 10 rad/s and 64 °C) was then calculated to evaluate the rutting
164 resistance for asphalt binders.

165 **Time Sweep (TS) fatigue test**

166 Under current specifications, the $G^*\cdot\sin\delta$ is used to classify the fatigue performance of
167 asphalt materials, which cannot effectively predict the fatigue resistance, especially for
168 the modified asphalt. With the 8-mm parallel plates, the control-displacement TS
169 fatigue tests were carried at 15°C, 19°C and 25°C, respectively. A single loading
170 frequency of 10 Hz with a strain amplitude of 2% was employed on the samples.
171 According to the previous researches of Wang (2016), the normalized dynamic shear
172 modulus ratio S is calculated as the following equation:

$$S = \frac{\left|G^*\right|}{\left|G^*\right|_{initial}} \tag{1}$$

173 Besides, the fatigue behaviors were evaluated from the perspective of energy

dissipation, the dissipation energy at *i*-the loading cycle w_i was expressed as following equation:

$$w_i = \pi\varepsilon\sigma\sin\delta = \pi\varepsilon^2 G^*\sin\delta \quad (2)$$

The cumulative dissipated energy ratio (DER) defined as the ratio between the cumulative dissipated energy up to *n*-the loading cycle and the dissipated energy at *n*-the cycle was calculated as following equation:

$$DER = \frac{\sum_{i=1}^{n} w_i}{w_n} \quad (3)$$

Where w_n is the dissipation energy at *n*-the loading cycle.

According to the method of Bonnetti (2002), a parameter of N_{p20} was developed as the fatigue life. It was widely accepted for evaluating the asphalt's fatigue behavior and defined as the number of loading cycles at which the DER curve deviates from the undamaged linear line (DER=N) by 20%.

The 50 percent reduction in undamaged $G^*(50\% G_0^*)$, peak in the $S \times N$ (where N is the number of loading cycles), and N_{p20} in DER-N curve was employed as the failure criteria. The equivalent fatigue life (N_f) was determined to evaluate the fatigue resistance of the asphalt binders.

Aging methods

In accordance with the JTG025-2000 Standard Test Methods of Bitumen and Bituminous Mixtures for Highway Engineering, the short-term aging was simulated by the Rolling Thin Film Oven Test (RTFOT) and Thin Film Oven Test (TFOT). By using the RTFOT samples, the asphalt binders were sustained the thermal-oxidative aging through the Pressure Aging Vessel (PAV) test to simulate the long-term aging. The RTFO test and PAV test for paving asphalts were both developed by the SHRP to simulate the thermal and oxidation aging in mixing plants and additional aging in

196 service.

197 **Single Edge Notched Beam (SENB) test**

198 The low temperature cracking resistance of asphalt binder is sensitive to the fracture
199 properties of asphalt materials. It has been reported that the SENB test can be used to
200 characterize the asphalt's cracking resistance, especially under the condition of large
201 strain (Hoare et al. 2000; Lei et al. 2015). By using the SENB device that was developed
202 by the Harbin Institute of Technology [**Fig. 1 (a)**], the fracture behaviors of asphalt
203 samples were evaluated at -12, -18 and -24°C. The span length L=110mm and the depth
204 of pre-notch a=2.8 mm. The SENB beam size is 12.7-mm width × 6.35-mm thickness
205 × 127-mm length. In this test, the loading with a rate of 0.05 mm/s was applied to the
206 top center of the beam. The program will automatically record the load and
207 displacement values with time. The schematic diagram of the SENB test is illustrated
208 in **Fig. 1(b)**.

209 In this study, the fracture load and fracture energy (G_f) were used for the evaluation of
210 the fracture behaviors of samples. The G_f is calculated as:

$$G_f = \frac{W_f}{A_{lig}} \tag{4}$$

211 Where $W_f = \int pdu$ is the total area under the entire load-deflection curve, p is the
212 applied force, u is the vertical displacement at the loading point, $A_{lig} = b(w-a)$ is the
213 area of the ligament, w=12.7 mm, b=6.35 mm.

214 **Fourier-transform Infrared Spectroscopy (FTIR) analysis**

215 As the indicators of chemical properties, the functional groups can be characterized in
216 terms of the infrared absorption spectrums by using the FTIR instrument (Dong et al.
217 2019; Yu et al. 2016). In this approach, the Nicolet is50 (**Fig. 2)** was carried out to
218 acquire the infrared spectrum of neat asphalt and polyurethane modified asphalt binders

from 4000 cm^{-1} to 500 cm^{-1} in ATR (Attenuated Total Reflection) mode.

Saturate, Aromatic, Resin, Asphaltene (SARA) fractions test

The compositions of asphalt binders are usually expressed in terms of the relative quantity percentages of the so-called SARA fractions for saturating, aromatic, resin, and asphaltene. The SARA fractions of base asphalt and PRM modified asphalts were separated by the Al_2O_3 chromatographic column method. Toluene, n-heptane and ethyl-alcohol were used for the separation.

Differential Scanning Calorimeter (DSC) characterization

The DSC test is a kind of thermo-analytical method which is developed to determine the physical changes of samples associated with a heat exchange under a controlled temperature. A 6-10 mg sample in the aluminum crucible was heated at a rate of 10°C/min from 0°C to 300°C, followed by the quenching process from 300°C down to 0°C at -10°C/min. The scans were then obtained by heating under the same conditions as the first stage. The T_g of asphaltene samples (**Fig. 3)** pre and after the modification was determined by using the NETZSCH 200F3 DSC manufactured in Germany. At least 3 duplicated samples were prepared and tested to ensure the accuracy of the test results.

Fluorescence Microscope (FM) analysis

Irradiated by the blue monochromatic light, the asphalt may emit an exceedingly small amount of fluorescence. However, for SBS and other polymer modifiers with spontaneous fluorescence properties, they may emit yellowish-green fluorescence that is visible to the human eyes. In this case, about 0.5g of fresh modified asphalt prepared with DS 70# neat asphalt was dropped onto a glass slide and heated in an oven at 145°C for 5min to make the asphalt droplet spread completely. The dispersive state of the

modifier was observed by the Olympus bx53 fluorescence microscope at room temperature (19°C), with 100 times magnification.

Atomic Force Microscopy (AFM) test

As a widely used technique for the investigation of micro-morphology of materials, the AFM (Model Dimension FastScan, Bruker Corporation, USA) was employed to study morphological characteristics of asphalts at micro-scale. Like the FM sample, about 0.5g fresh liquid asphalt samples wad carefully dropped on the glass slides and kept at 145°C for 5 minutes to form films. The samples were then cooled to room temperature (20°C) for the investigation of morphology by the AFM using tapping mode.

Results and discussion

Complex shear modulus (G) and phase angle (δ)*

The G^* and δ master curves for all the investigated samples are illustrated in **Fig. 4** and **5**, respectively. According to the master curves, there is a significant increase of G^* and decrease of δ with increasing PRM concentration at low frequencies, which indicates that the addition of PRM improves the high-temperature elasticity and rutting-resistance for the asphalt binders. The G^* and δ master curves of PRM modified asphalt (at 1.5%, 2.5 and 4%) are close to that of base asphalt at the high frequencies. In terms of the δ master curves, a slight plateau presents at frequencies approximately from 10^{-4} to 10^{-1} Hz for the PRM modified asphalt. As an indicator of elastic networks with entanglements, this result provides additional evidence for the formation of the crosslinking network formed in the PRM modified asphalt. Besides, the master curves for PMAs extend over a smaller span of frequency compared with those for neat DS 70# asphalt binder. This indicates that the temperature susceptibility of the asphalt binder is reduced due to the incorporation of PRM.

267 ***High-temperature performance***

268 In order to clarify the effect of modification with PRM on the high-temperature
269 performance of asphalt, the universal Superpave rutting parameter G*/sin δ of the neat
270 asphalt and modified asphalt under unaged, TFOT, RTFOT and PAV aging conditions
271 were investigated. **Fig. 6** illustrates the result for the neat asphalt and PRM modified
272 asphalt binders. It is obvious that the G*/sin δ increases with the increase of PRM
273 concentration regardless of the aging conditions. The PRM modified asphalt with 4 %
274 PRM modifier has the highest G*/sin δ values in all cases. The result indicates that the
275 permanent deformation resistance of PRM modified asphalt is significantly improved.
276 In addition, the G*/sin δ values of all test samples are greater than 1.00 kPa according
277 to Superpave specification. In the following section, the aging properties of binders will
278 be further investigated.

279 ***Low-temperature performance***

280 **Fig. 7** illustrates the load-deflection curves from the SENB test at -18°C. As can be
281 seen, the incorporation of PRM has a significant influence on deformation ability. The
282 addition of PRM may improve the stiffness modulus of asphalt. With the increase of
283 the modifier content, the fracture load and fracture deformation increase first and then
284 decrease.

285 According to the theory of material damage, cracking is regarded to occur when the
286 accumulated energy is greater than the critical limit. In this regard, the index of fracture
287 energy was used to characterize the low-temperature cracking performance of samples.
288 By using the load-deflection curves from the SENB test, the fracture energy for the neat
289 and PMAs at -12 to 24°C was investigated, as illustrated in **Fig. 8**. It was observed that
290 the modification can result in higher fracture energy. Meanwhile, the fracture energy

increases first and then decreases with the increased PRM concentration. The result indicates the low temperature cracking resistance is improved. This may attribute to the beneficial effect of the crosslinking network formed in the PRM modified asphalt. However, due to the limited scale and mechanical strength of crosslinking, its contribution to cracking resistance is limited. Besides, the increases of PRM concentration leads to the further separation of heavy domains and maltene as seen in a comparison of AFM images, which not only reduces the fracture toughness of asphalt binder, but also make the micro-cracks easy to develop at the domain boundaries because of stress concentration. Due to the combined effects of the above two factors, the fracture energy may be reduced by very high concentrations of PRM modifier. Thus, cautions must be taken when excessive PRM modifiers are incorporated.

Fatigue properties

Based on the previously introduced fatigue criteria, the comparisons of the fatigue lives of all the asphalt samples in TS test were determined and are listed in **Table 2**. It can be observed that the temperature has s significant effect on fatigue lives. Although the trends in fatigue life with varying temperature is quite a binder dependent, it can be observed that the incorporation of PRM significantly increases the fatigue life of neat asphalt at the three selected test temperatures, which indicates the modification with PRM significantly improves the binder's resistance to fatigue damage. Besides, concerning the effect of PRM on the asphalt's fatigue resistance, all the applied three failure definitions showed good consistence. The addition of PRM improves the stiffness of the asphalt binder, but reduces the fatigue susceptibility. As a result, the service life of asphalt pavement is expected to be improved by the PRM modified asphalt.

315 ***Aging properties***

316 The Christensen-Anderson-Marasteanu (CAM) model are employed to characterize the
317 G*and δ master curves (Zeng et al. 2001), as follows:

$$G^* = \frac{G_g}{[1+(f_c/\alpha_T f)^k]^{m_e/k}} \quad (5)$$

$$\delta = \frac{90 m_e}{1+(f_c/f)^k} \quad (6)$$

318 Where f is the loading frequency, f_c is a location parameter, G_g is the glassy shear
319 modulus; k and m_e is a dimensionless shape parameter and α_T is the shift factor that is
320 related to the WLF equation.

321 As an example, **Fig. 9** illustrates the G* master curves of neat asphalt before and after
322 PAV aging at 36°C. According to the method proposed by Cavalli et al. (2018), the
323 rheological aging index (*RAI*) was calculated according to the area between the G*
324 master curves in the log-log scale.

325 In this research, the unified reduced frequency limits from 10^{-4} to 10^4 was selected for
326 the evaluations of all the aging effects, according to the following equation (7):

$$RAI = \frac{\int_{-4}^{4}[\log|G^*|(\tilde{\xi}_{aged}) - \log|G^*|(\tilde{\xi}_{unaged})]d\xi}{\int_{-4}^{4}\log|G^*|(\tilde{\xi}_{unaged})d\xi} \quad (7)$$

327 where, |G*| is the complex modulus and ξ is the logarithm of the reduced frequency
328 between the integral limits. A lower *RAI* value represents a better aging resistance.

329 The *RAI*s of investigated asphalt samples are presented in **Fig. 10**. As can be seen,
330 thermo-oxidative aging shows a significant influence on the aging behavior of asphalt
331 binders. The *RAI* of aged neat asphalt are all higher than that of the PRM modified
332 asphalt under the same aging condition, which implies the aging resistance of PRM
333 modified asphalt is better than the neat asphalt. Meanwhile, it could be found that the
334 aging degree of PRM modified asphalt decreases when more PRM is added. By

335 comparing the *RAI*s between the TFOT and RTFOT aged samples, it can be seen that
336 deference was magnified at high PRM concentration. During the aging process, the
337 carbonyl compounds that formed from the phenols and benzyl alcohols in PRM
338 modified asphalt are expected to be reduced. The number of potential sites for thermal-
339 oxidation aging is reduced, which weakens the transfer of light components to heavy
340 components to a certain extent. Thus, the aging degree of PRM modified asphalt is less
341 than that of unmodified asphalt. Besides, since the RTFOT is regarded as a more
342 effective approach to simulate the degradation of asphalt that occurs during the hot-mix
343 process, the result further emphasized the importance of using RTFOT to simulate the
344 short-time thermal-oxidative aging of PRM modified asphalt.

345 ***SARA fractions analysis***

346 The evolution of SARA fractions is illustrated in **Fig. 11**. By using the colloidal index
347 (I_c), the colloidal state of asphalt binders was further evaluated. The I_c was originally
348 introduced by Baginska and Gaestel et al. (2004), and calculated in terms of the SARA
349 fractions, as shown in the following equation:

$$I_C = \frac{Asphaltenes + Saturates}{Aromatics + Resins} \tag{8}$$

350 As can be seen, the addition of PRM leads to a significant increase in the fraction of the
351 asphaltenes and a reduction of the resins. The percentage of asphaltenes increased from
352 11.7% in base asphalt to 20.0% in 4% PRM modified asphalt. The percentage of resins
353 decreased from 32.6% in base asphalt to 26.4% in 4% PRM modified asphalt. As
354 previously mentioned, the polar groups mainly exist in the asphaltenes and resins, this
355 result suggest that incorporation of PRM may lead to the consumption of resins and the
356 re-configuration of asphaltenes. As a result, the PRM modified asphalt presents higher

I_c with increasing PRM concentrations, which indicates the evolution of colloid structure from sol type or sol-gel to gel type.

FTIR analysis

To highlight the product of modification, the PRM modified asphalt with high PRM percentage of 2.5% were prepared for the FTIR investigation. The FTIR spectrums for the neat asphalt and PRM modified asphalt are illustrated as absorbance against wavenumber. The absorbance spectrums for the investigated samples are superimposed on each other for a better comparison of the evolutions of functional groups, as presented in **Fig. 12**.

In terms of the PRM modified asphalt, the locations of its major absorption bands appeared are similar to those of neat asphalt. No absorption peak at 2270 cm^{-1} due to ν_{as} (NCO) was observed in the spectrum of the PRM modified asphalt, which indicates the isocyanate group in PRM was fully consumed. However, peak at 1650 cm^{-1} implying the stretching vibration of C=O (amide-I) are noticed after modification, which does not appear in either neat asphalts or PRM modifier. This may suggest the generation of substituted urea bonds by -NH_2 /-NH groups in neat asphalt and –NCO group in PRM modifier, as illustrated in Reaction (1)-(2).

$$\text{R-NCO + R'R"-NH} \rightarrow \text{R-NH-CO-N-R'R"} \quad (1)$$

$$\text{R-NCO + R'-NH}_2 \rightarrow \text{R-NH-CO-NH-R'} \quad (2)$$

Besides, the two bands at 1511, 1310 can be attributed to δ(NH) with ν(CO-N) (amide-II) and ν(C-N) with δ(NH) (amide-III) in urethane linkages, respectively. This indicates that a higher number of urethane bonds are activated due to the reaction between the -OH group of neat asphalt and –NCO group of PRM modifier, as illustrated in Reaction (3).

$$R\text{-}NCO + R'\text{-}OH \rightarrow R\text{-}NH\text{-}CO\text{-}O\text{-}R' \quad (3)$$

Accordingly, the FTIR spectrums directly reveal the formation of new urethane-derived and urea- derived compounds in the PRM modified asphalts. Among the active groups in asphalt that can react with the isocyanate functional groups, the pyridine, pyrrole, indole, phenol functional groups play important roles. As a result, the modification using PRM modifier leads to a steadier internal structure and superior high-temperature performance.

DSC analysis

As a multi-component mixture, the compositions of asphalt can be simply classified in terms of two phases: the asphaltene phase and the maltene phase. The maltene phase is further separated into sub-fractions of saturates, aromatics, and resins. The additional SARAs test was performed to check the evolutions of asphalt fractions. The SARA fractions of saturating, aromatic, resin, asphaltene for the 2.5% PRM modified asphalt binder is 16.1%, 21.1%, 32.8% and 28.9%, respectively. The addition of PRM leads to a significant increase in the fraction of the asphaltenes and a reduction of the resins, which implies the PMA binder is harder than the neat asphalt binder. As the heaviest fraction in asphalt, the asphaltene plays an important role in the evolution of asphalt structures.

As mentioned, the repeated DSC scan was conducted on the asphalt samples. Zhang et. al (2005) pointed out that the evaporation of light components and the melting of some components in asphaltene occurred during heating to 300°C. The second DSC scan is recommended to be used to determine the thermal properties of the asphaltene since the overlapping effects in the first scan may result in inaccurate information. The DSC curves of the asphaltenes that extracted from the neat asphalt and 2.5% PRM modified asphalt are illustrated in **Fig. 13**.

According to the result of T_g analysis form the heat flow curves, the PRM had two effects. It leads to an obvious increase of T_g and a significantly upward baseline shift of the DSC curve. This result indicates the loss in molecular motion and change of assembling structures. Generally, restricted molecular motions can be caused by the bridging of neighboring molecules (cross-linking), a loss of plasticizer (e.g., an oil), or greater intermolecular interactions due to ionic or hydrogen bonds (Masson et al. 2010; Mark et al. 1993). This result is correlated with the improvement of the high-temperature performance of the PMAs.

FM analysis

At the initial stage of the observation, about 0.5g PRM modifier was dropped onto the surface of neat asphalt and observed for the comparison of fluorescence characteristics. The comparison results are shown in **Fig.14 (a)**. It can be found that the PRM exhibits obvious yellowish-green fluorescence. The FM image of PRM modified asphalt is presented in **Fig.14(b)-(d).** Obviously, no phase segregation or modifier aggregation was found. The result proved that the PRM has good compatibility with neat asphalt, which is conducive to the formation of a stable structure for the blending system.

AFM analysis

Fig.15 illustrates the micrographs captured by the AFM corresponding to the DS 70# base asphalt and PRM modified asphalts. The scanning area is 30×30 um and the testing temperature is 20°C. As can be seen in **Fig.15(a)**, bee-like (black with white streaks) type structures (catanaphase) have appeared in the neat asphalt, which is commonly regarded to be caused by the presence of asphaltenes and waxes in the asphalt (Pauli et al. 2011; Lyne et al. 2013). After the incorporation of a 1.5% PRM modifier into the base asphalt [**Fig.15(b)**], it is found that the sharp size of catanaphase is increased,

together with the increase of interactions. Upon an increase to 4% PRM [**Fig.15(d)**], the crosslinking network shows an obvious enhancement. In this case, the incorporation of PRM could increase the asphaltene domain and reduce the thermal susceptibility of asphalts, resulting in an improvement of high-temperature performance.

With respect to the depression phases in the AFM images, the catanaphase in neat asphalt contrasted lightly against the matrix. When 1.5% PRM was added, the contrast increased significantly. With 2.5% and 4% PRM, the domain of the paraphase (lightly shaded) was further dispersed into multiple smaller domains. Since the periphase (dark shaded) and the farther paraphase were respectively attributed to mixed resins and aromatics (Masson et al. 2010), the increased segregation of maltene and catanaphase may attribute to the evolution of selective aggregation between interacting phases.

Conclusions and Outlook

This research investigated the effectiveness of using a polyurethane-precursor-based reactive modifier (PRM) to improve asphalt performance. The pavement performance, morphology characteristics, FTIR spectrums, thermal properties were obtained. Based on the works mentioned above, some crucial conclusions can be drawn:

1. The G^* and δ master curves, Superpave rutting parameter, TS and SENB test results show that the incorporation of the employed PRM can significantly improve the high-temperature rutting resistance, fatigue resistance and low-temperature cracking resistance of asphalt binders. Cautions must be taken when excessive PRM modifier is incorporated since the low-temperature cracking resistance may be reduced by too high concentrations of PRM.
2. By the aid of G^* master curves, the rheological aging index (*RAI*) shows that the PRM modified asphalt has better aging resistance than the neat asphalt. It may be related to the decrease of active sites (such as phenols and benzyl alcohols) of

molecules during modification.

3. According to the evolution of SARA fractions, the incorporation of PRM modifier may promote the transition from resin to asphaltene by the chemical bonding, and thus leading to superior high temperature performance.
4. The FTIR investigations reveal that the chemical groups of urethane and urea were generated during the modification with the employed PRM. Thus, the chemical linkages constructed between the PRM and asphalt fractions may lead to a steadier internal polymeric structure and superior high-temperature performance for the asphalt.
5. The FM and AFM reveal the micromorphology of PRM modified asphalt. The FM analysis shows excellent compatibility between the neat asphalt and PRM. The AFM analysis reveals the segregation of maltene and asphaltene. It emphasizes the importance of asphaltene in the construction of crosslinking networks in the PRM modified asphalt.

Overall, the PRM modified asphalt presents superior high-temperature rutting resistance and desirable low-temperature crack resistance, fatigue resistance and aging resistance. It is an ideal modifier for asphalt binders, especially suitable for high-temperature regions. Moreover, the production temperature of PRM modified asphalt can be carried out at 145°C, which is much lower than that of the traditional polymer modified asphalt. The objective of this research is to evaluate the pavement performance and modification mechanism of the asphalt binders modified with a novel polyurethane-precursor-based reactive modifier. Therefore, the research work is carried out based on the comparison with the neat asphalt. The feasibility of the PRM modifier will be further clarified by comparing it with the SBS modified asphalt.

Data Availability Statement

All data and models generated or used during the study appear in the published article.

Acknowledgments

The financial supports from National Key Research and Development Program of China (2018YFB1600100) and Natural Science Foundation of Heilongjiang Province of China (JJ2020ZD0015) are gratefully acknowledged. The authors are solely responsible for the content.

Reference

Airey, G. D. 2002. Rheological evaluation of ethylene vinyl acetate polymer modified bitumens. *Construction and Building Materials*. 16(8): 473-487. https://doi.org/10.1016/S0950-0618(02)00103-4.

Ali, S. I. A. , Ismail, A. , Yusoff, N. I. M. , Karim, M. R. , Al-Mansob, R. A. and Alhamali, D. I. 2015. Physical and rheological properties of acrylate–styrene–acrylonitrile modified asphalt cement. *Construction and Building Materials*. 93: 326-334. https://doi.org/10.1016/j.conbuildmat.2015.05.016.

Baginska, K. and Gawel, I. 2004. Effect of origin and technology on the chemical composition and colloidal stability of bitumens. *Fuel Processing Technology*. 85(13): 1453-1462. https://doi.org/10.1016/j.fuproc.2003.10.002

Baumgardner, G. L. , Masson, J. F. , Hardee, J. R. , Menapace, A. M. and Williams, A. G. 2005. Polyphosphoric acid modified asphalt: proposed mechanisms. In Vol. 74 of *Proc., Technical Session of the Association of Asphalt Paving Technologists*, 283-305. Minnesota: Assoc Asphalt Paving Technologists.

Bineet Baliyar Singh, Fanismita Mohanty, Sudhanshu Sekhar Das, Sarat Kumar Swain. Graphene sandwiched crumb rubber dispersed hot mix asphalt[J]. *Journal of Traffic and Transportation Engineering (English Edition)*,2020, 7 (5): 652-667.

Bonnetti, K. , Nam, K. and Bahia, H. 2002. Measuring and defining fatigue behavior of asphalt binders. Transportation Research Record *Journal of the Transportation Research Board*. 1810(1): 33-43. https://doi.org/10.1016/j.fuproc.2003.10.002

Cavalli, M. C., Zaumanis, M., Mazza, E., Partl, M. N. and Poulikakos, L. D. 2018. Effect of ageing on the mechanical and chemical properties of binder from rap treated with bio-based rejuvenators. *Composites Part B Engineering*. 141: 174-181. https://doi.org/ 10.1016/j.compositesb.2017.12.060.

Carrera, V. , Partal, P. , M. Garcia-Morales, Gallegos, C. and A. Perez-Lepe. 2010. Effect of processing on the rheological properties of poly-urethane/urea bituminous products. *Fuel Processing Technology*. 91(9): 1139-1145. https://doi.org/ 10.1016/j.fuproc.2010.03.028.

Carrera, V. , Partal, P. , García-Moralés, M. , Gallegos, C. and Paez, A. 2009. Influence of bitumen colloidal nature on the design of isocyanate-based bituminous products with enhanced rheological properties. *Industrial & Engineering Chemistry Research*. 48(18): 8464-8470. https://doi.org/ 10.1021/ie9004404.

Carrera, V. , García-Morales, M. , Partal, P. and Gallegos, C. 2010. Novel bitumen/isocyanate-based reactive polymer formulations for the paving industry. *Rheologica Acta*. 49(6): 563-572. https://doi.org/10.1021/ie9004404.

Dong, Z. J., Zhou, T., Luan, H., Williams, R. C., Wang, P. and Leng, Z. 2019. Composite modification mechanism of blended bio-asphalt combining styrene-butadiene-styrene with crumb rubber: A sustainable and environmental-friendly solution for wastes. *Journal of Cleaner Production*. 214: 593-605. https://doi.org/ 10.1016/j.jclepro.2019.01.004.

Fang, C. , Yu, X. , Yu, R. , Liu, P. and Qiao, X. 2016. Preparation and properties of isocyanate and nano particles composite modified asphalt. *Construction and Building Materials*. 119: 113-118. https://doi.org/10.1016/j.conbuildmat.2016.04.099 .

Pahlavan, F. , Samieadel, A. , Deng, S. and Fini, E. H. 2019. Exploiting synergistic effects of intermolecular interactions to synthesize hybrid rejuvenators to revitalize aged asphalt. *ACS Sustainable Chemistry & Engineering*. 7: 15514−15525. https://doi.org/10.1021/acssuschemeng.9b03263

Hoare, T. R. and Hesp, S. A. 2000. Low-temperature fracture testing of asphalt binders: regular and modified systems. *Transportation Research Record*. 1728(1) : 36-42. https://doi.org/ 10.3141/1728-06.

Khabaz, F. and Khare, R. 2015. Glass transition and molecular mobility in styrene-

butadiene rubber modified asphalt. *Journal of Physical Chemistry B*. 119(44) : 14261-9. https://doi.org/10.1021/acs.jpcb.5b06191.

Lei, Z., Bahia, H. and Yi-qiu, T. 2015. Effect of bio-based and refined waste oil modifiers on low temperature performance of asphalt binders. *Construction and Building Materials*. 86: 95-100. https://doi.org/10.1016/j.conbuildmat.2015.03.106.

Li, T., Lu, G., Wang, D., Hong, B., Tan, Y.Q. and Oeser, M., 2019. Key properties of high-performance polyurethane bounded pervious mixture. *China Journal of Highway and Transport*, 32(4), pp.158-169.

Li, X. , Zhou, Z. and You, Z. 2016. Compaction temperatures of sasobit produced warm mix asphalt mixtures modified with sbs. *Construction and Building Materials*. 123: 357-364. https://doi.org/ 10.1016/j.conbuildmat.2016.07.015.

Liang, M. , Ren, S. , Fan, W. , Xin, X. , Shi, J. and Luo, H. 2017. Rheological property and stability of polymer modified asphalt: effect of various vinyl-acetate structures in eva copolymers. *Construction and Building Materials*. 137: 367-380. https://doi.org/ 10.1016/j.conbuildmat.2017.01.123.

Liu, H. , Zhang, M. , Wang, Y. , Chen, Z. and Hao, P. 2018. Rheological properties and modification mechanism of polyphosphoric acid-modified asphalt. *Road Materials and Pavement Design*. 21(4), 1-18. https://doi.org/ 10.1080/14680629.2018.1537931

Lu, G., Renken, L., Li, T., Wang, D., Li, H. and Oeser, M., 2019. Experimental study on the polyurethane-bound pervious mixtures in the application of permeable pavements. *Construction and Building Materials*, 202, pp.838-850.

Lu, X. and Isacsson, U. 1998. Chemical and rheological evaluation of ageing properties of sbs polymer modified bitumens. *Fue*. 77(9): 961-972.

Lv, S., Liu, C., Yao, H. and Zheng, J. 2018. Comparisons of synchronous measurement methods on various moduli of asphalt mixtures. *Construction and Building Materials*. 158: 1035-1045. https://doi.org/10.1016/S0016-2361 (97)00283- 4.

Lyne, Å. L. , Wallqvist, V. and Birgisson, B. 2013. Adhesive surface characteristics of bitumen binders investigated by atomic force microscopy. *Fuel*. 113: 248-256. https://doi.org/ 10.1016/j.fuel.2013.05.042.

M.J. Martín-Alfonso, Partal, P. , Navarro, F. J. , M. García-Morales, Bordado, J. C. M.

568 and Diogo, A. C. 2009. Effect of processing temperature on the bitumen/mdi-peg
569 reactivity. *Fuel Processing Technology*. 90(4): 525-530. https://doi.org/
570 10.1016/j.fuproc.2009.01.007.

571 Mark J. E. ,Eisenberg A. ,Graessley W. W. ,Mandelkern L. , Samulski E. T. ,Koenig J.
572 L. and Wignall G. D. 1993. The Glassy State and the Glass Transition, in Physical
573 Properties of Polymers, American Chemical Society, Washington, D.C., 2nd ed.
574 https://doi.org/10.1017/CBO9781139165167.003

575 Masson, J. F. , Leblond, V. , Margeson, J. and Bundalo-Perc, S. 2010. Low-temperature
576 bitumen stiffness and viscous paraffinic nano- and micro-domains by cryogenic
577 afm and pdm. *Journal of Microscopy*. 227(3): 191-202. https://doi.org/
578 10.1111/j.1365-2818.2007.01796.x

579 Mousavi, M. and Fini, E. H. 2019. Moderating effects of paraffin wax on interactions
580 between polyphosphoric acid and bitumen constituents. *ACS Sustainable*
581 *Chemistry & Engineer*ing. 7(24): 19739–19749. https://doi.org/
582 10.1021/acssuschemeng.9b05008

583 Navarro, F. J., Martínez-Boza, F. J., Partal, P., Gallegos, C., Munoz, M. E., Areizaga, J.
584 and Santamaría, A. 2001. Effect of processing variables on the linear viscoelastic
585 properties of SBS-oil blends. *Polymer Engineering & Science*. 41(12): 2216-2225.
586 https://doi.org/ 10.1002/pen.10917.

587 Pauli, A. T. , Grimes, R. W. , Beemer, A. G. , Turner, T. F. and Branthaver, J. F. 2011.
588 Morphology of asphalts, asphalt fractions and model wax-doped asphalts studied
589 by atomic force microscopy. *International Journal of Pavement Engineering*.
590 12(4): 291-309. https://doi.org/ 10.1080/10298436.2011.575942.

591 Presti, L. and Davide. 2013. Recycled tyre rubber modified bitumens for road asphalt
592 mixtures: a literature review. *Construction and Building Materials*. 49: 863-881.
593 https://doi.org/ 10.1016/j.conbuildmat.2013.09.007.

594 Richard Y. Ji, Tirupan Mandal, Hao Yin. Laboratory characterization of temperature
595 induced reflection cracks[J]. *Journal of Traffic and Transportation Engineering*
596 *(English Edition)*,2020, 7 (5): 668-677.

597 Shadmani, A., Tahmouresi, B., Saradar, A. and Mohseni, E. 2018. Durability and
598 microstructure properties of SBR-modified concrete containing recycled asphalt
599 pavement. *Construction and Building Materials*. 185: 380-390.

https://doi.org/10.1016/j.conbuildmat.2018.07.080.

Shi, L. W., Wang, D. Y., Masley, J. and Zhang, S. W. 2014. Comparison Analysis of the Aggregate Contact Characteristics between Skeleton-Dense and Suspended-Dense Structure Asphalt Mixture. *In Applied Mechanics and Materials*. 470: 889-892. https://doi.org/ 10.4028/www.scientific.net/AMM.470.889.

Singh, B. , Tarannum, H. and Gupta, M. 2003. Use of isocyanate production waste in the preparation of improved waterproofing bitumen. *Journal of Applied Polymer Science*. 90(5): 13. https://doi.org/ 10.1002/app.12808.

Wang, C., Zhang, H., Castorena, C., Zhang, J. and Kim, Y. R. 2016. Identifying fatigue failure in asphalt binder time sweep tests. *Construction and Building Materials*. 121(SEP.15), 535-546. https://doi.org/10.1016/j.conbuildmat.2016.06.020.

Wei, J., Liu, Z. and Zhang, Y. 2013. Rheological properties of amorphous poly alpha olefin (APAO) modified asphalt binders. *Construction and Building Materials*. 48: 533-539. https://doi.org/10.1016/j.conbuildmat.2013.07.087.

Wekumbura, C. , Stastna, J. and Zanzotto, L. 2007. Destruction and recovery of internal structure in polymer-modified asphalts. *Journal of Materials in Civil Engineering*. 19(3): 227-232. https://doi.org/ 10.1061/(ASCE)0899-1561(2007)19: 3(227).

Xia, L. , Cao, D. , Zhang, H. and Guo, Y. 2016. Study on the classical and rheological properties of castor oil-polyurethane pre-polymer (c-pu) modified asphalt. *Construction and Building Materials*. 112: 949-955. https://doi.org/ 10.1016/j.conbuildmat.2016.02.207.

Xiao, F., Amirkhanian, S., Wang, H. and Hao, P. 2014. Rheological property investigations for polymer and polyphosphoric acid modified asphalt binders at high temperatures. *Construction and Building Materials*. 64: 316-323. https://doi.org/ 10.1016/j.conbuildmat.2014.04.082.

Xu, X., Leng Z., Lan J., Wang W., Yu J., Bai Y., Sreeram A. and Hu, J. 2020. Sustainable practice in pavement engineering through value-added collective recycling of waste plastic and waste tyre rubber. *Engineering*. https://doi.org/10.1016/j.eng.2020.08.020.

Yang, X. , Mills-Beale, J. and You, Z. 2017. Chemical characterization and oxidative aging of bio-asphalt and its compatibility with petroleum asphalt. *Journal of Cleaner Production*. 142: 1837-1847. https:// doi.org/10.1016/j.jclepro.2016.11.

100.

Yin, W. , Ye, F. and Lu, H. 2017. Establishment and experimental verification of stability evaluation model for sbs modified asphalt: based on quantitative analysis of microstructure. *Construction and Building Materials*. 131: 291-302. https:// doi.org/10.1016/j.conbuildmat.2016.11.041.

Yu, R. , Zhu, X. , Zhou, X. , Kou, Y. and Fang, C. 2017. Rheological properties and storage stability of asphalt modified with nanoscale polyurethane emulsion. *Petroleum Science and Technology*. 36(1): 1-6. https://doi.org/ 10.1080/10916466. 2017.1405028.

Yu, H. , Leng, Z. , Xiao, F. and Gao, Z. 2016. Rheological and chemical characteristics of rubberized binders with non-foaming warm mix additives. *Construction and Building Materials*. 111: 671-678. https://doi.org/10.1016/j.conbuildmat. 2016.02.066.

Yuliestyan, A., Cuadri, A. A., García-Morales, M. and Partal, P. 2016. Binder design for asphalt mixes with reduced temperature: eva modified bitumen and its emulsions. *Transportation Research Procedia*. 14: 3512-3518. https://doi.org/ 10.1016/j.trpro.2016.05.319.

Zhang, K. and Kevern, J. 2021. Review of porous asphalt pavements in cold regions: the state of practice and case study repository in design, construction, and maintenance. *Journal of Infrastructure Preservation and Resilience*. 2(1). https://doi.org/10.1186/s43065-021-00017-2.

Zeng, M. , Bahia, H. U. , Zhai, H. , Anderson, M. R. and Turner, P. 2001. Rheological modeling of modified asphalt binders and mixtures. *Asphalt Paving Technology: Association of Asphalt Paving Technologists-Proceedings of the Technical Sessions*. 70(1): 403-441. https://doi.org/ 10.1016/j.jpainsymman.2008.02.002.

Zhang, F. and Yu, J. 2010. The research for high-performance SBR compound modified asphalt. *Construction and Building Materials*. 24(3): 410-418. https://doi.org/ 10.1016/j.conbuildmat.2009.10.003.

Zhang, Y. , Takanohashi, T. , Shishido, T. , Sato, S. , Saito, I. and Tanaka, R. 2005. Estimating the interaction energy of asphaltene aggregates with aromatic solvents. *Energy & Fuels*. 19(3): 1023-1028. https://doi.org/10.1021/ef0498770

664 **Table 1** Physical properties of the base asphalt

Physical properties	DS 70#	Specification
Penetration @25°C (0.1 mm)	67.7	T 0604-2011
Ductility @15°C and 5 cm/min (cm)	>100	T 0605-2011
Softening point (°C)	48.9	T 0606-2011
Brookfield viscosity @135°C (Pa·s)	0.383	T 0625-2011
Brookfield viscosity @175°C (Pa·s)	0.084	T 0625-2011
SARAs component (weight %)		
Saturates	20.93	T 0618-2011
Aromatics	34.82	
Resins	32.56	
Asphaltene	11.69	

665

666 **Table 2** Fatigue lives determined from different failure criteria.

Temperature (°C)	Asphalt binder	Fatigue lives from multiple failure definitions		
		50% G_0^*	Max $S \times N$	DER (N_{p20})
15	DS 70#	61581	43808	52617
	DS+1.5%	163340	129387	129446
	DS+2.5%	213203	173894	189472
	DS+4%	363972	291368	302872
19	DS 70#	48863	35398	34142
	DS+1.5%	116180	84070	85054
	DS+2.5%	245301	181662	190389
	DS+4%	398415	334940	309268
25	DS 70#	44614	33590	31258
	DS+1.5%	100819	76854	77280
	DS+2.5%	224458	164541	170576
	DS+4%	684302	595712	547379

667

668 **Figure Captions List**

669
670 (a)

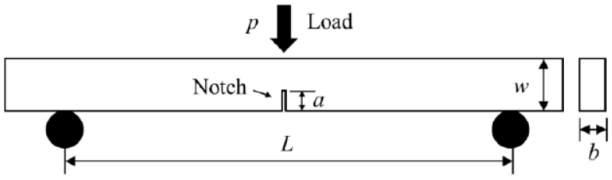

671
672 (b)

673 **Fig. 1.** The illustration of SENB test. (a) The SENB device. (b) The loading schematic

674 diagram.

675
676 **Fig. 2.** The FTIR device with ATR module.

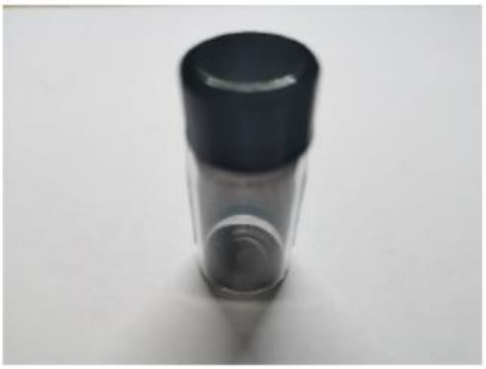

677
678 **Fig. 3.** The asphaltene samples obtained from the SARA test.

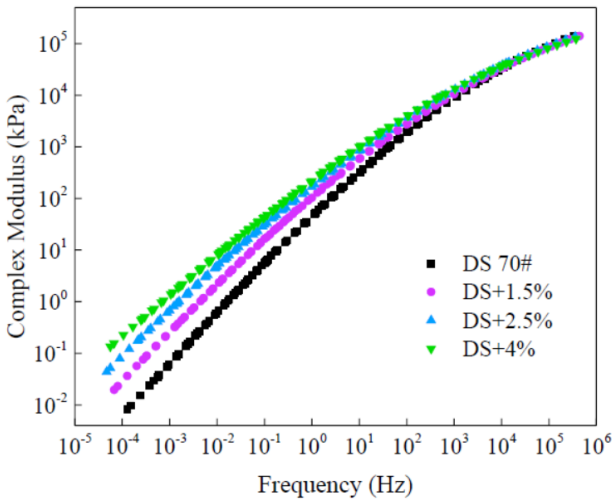

Fig. 4. The *G** master curves for the neat and PRM modified asphalt binders.

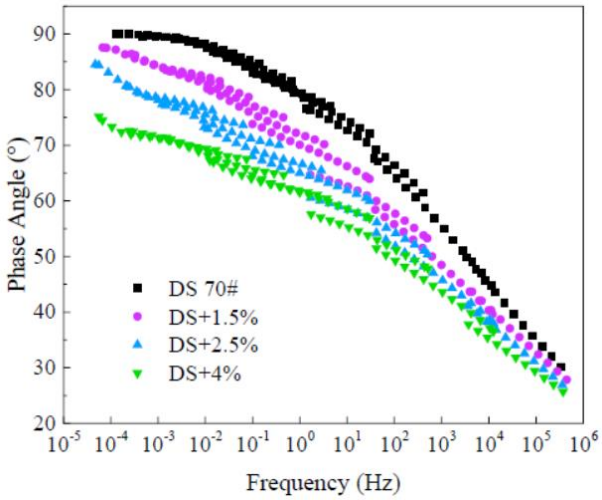

Fig. 5. The δ master curves for the neat and PRM modified asphalt binders.

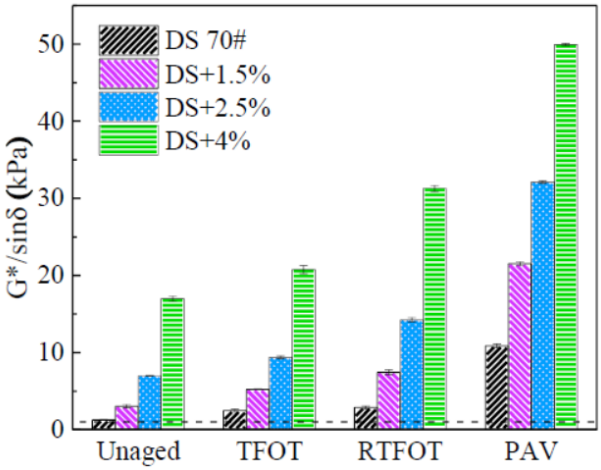

Fig. 6. The rutting parameter G*/sinδ for the neat and PRM modified asphalt binders.

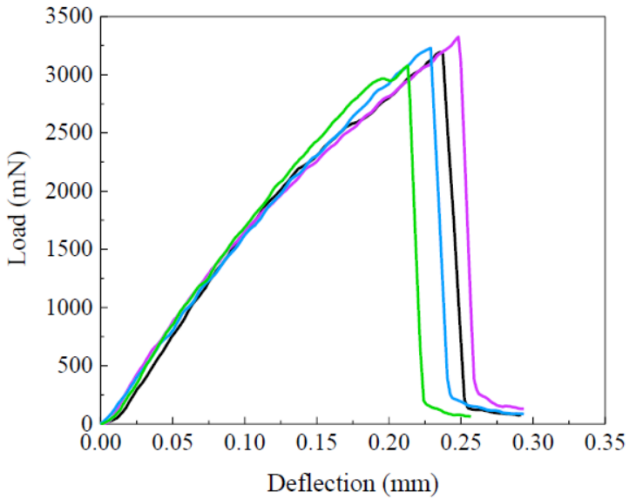

685
686 **Fig. 7.** The SENB load-deflection curves for the neat and PRM modified asphalt

687 binders at -12°C.

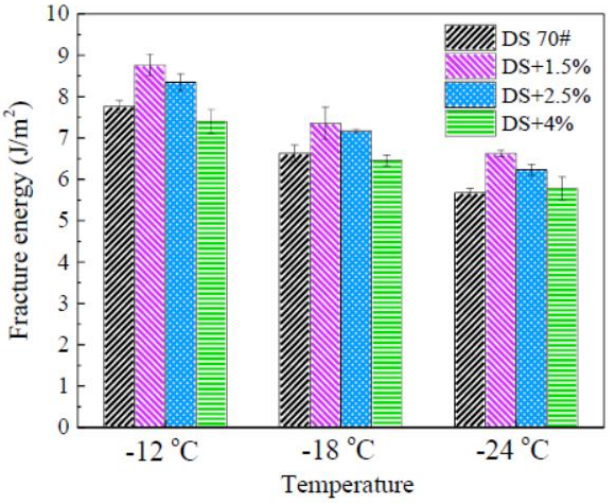

688
689 **Fig. 8**. The fracture energy for the neat and PRM modified asphalt binders.

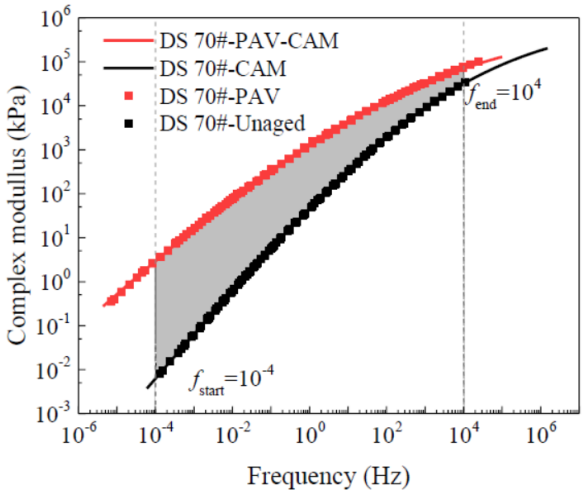

690
691 **Fig. 9.** The illustration of the calculation of *RAI*.

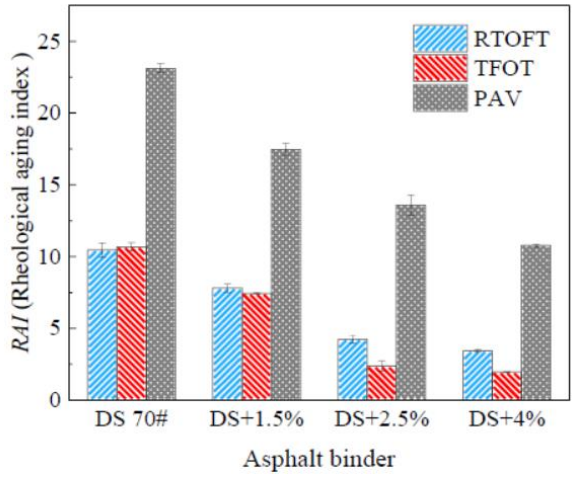

692
693 **Fig. 10.** The *RAI* for the neat and PRM modified asphalt binders.

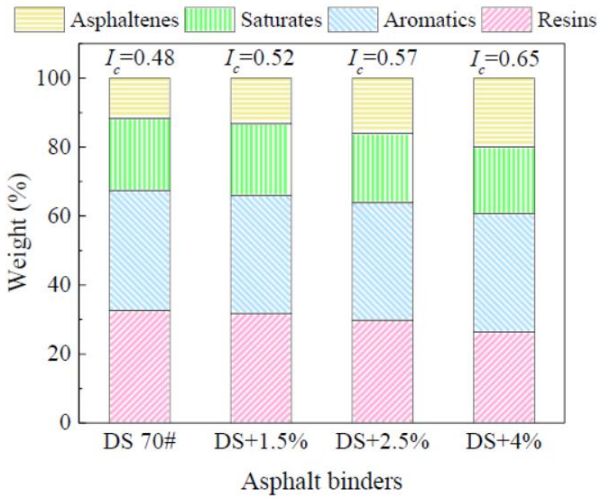

694
695 **Fig. 11.** The SARA fractions for the neat and PRM modified asphalt binders.

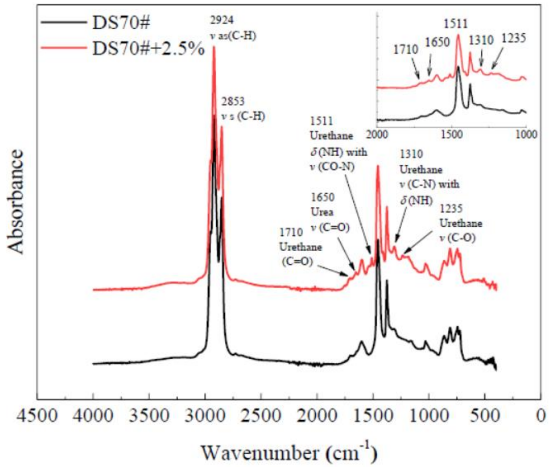

696
697 **Fig. 12.** The infrared spectrums for the neat and PRM modified asphalt binders.

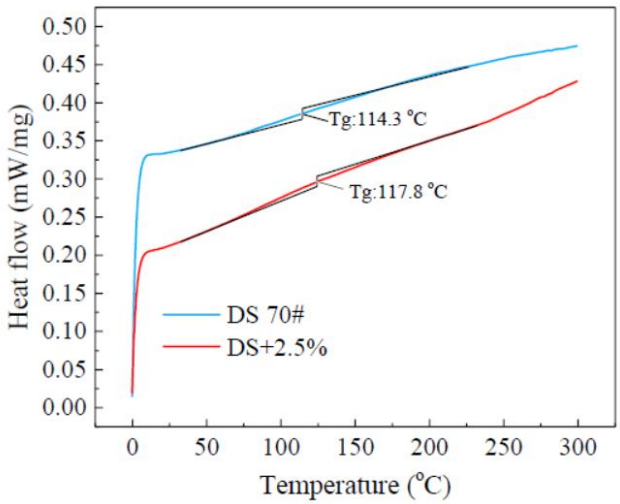

Fig. 13. The DSC curves for the asphaltenes of the neat and PRM modified asphalt binders.

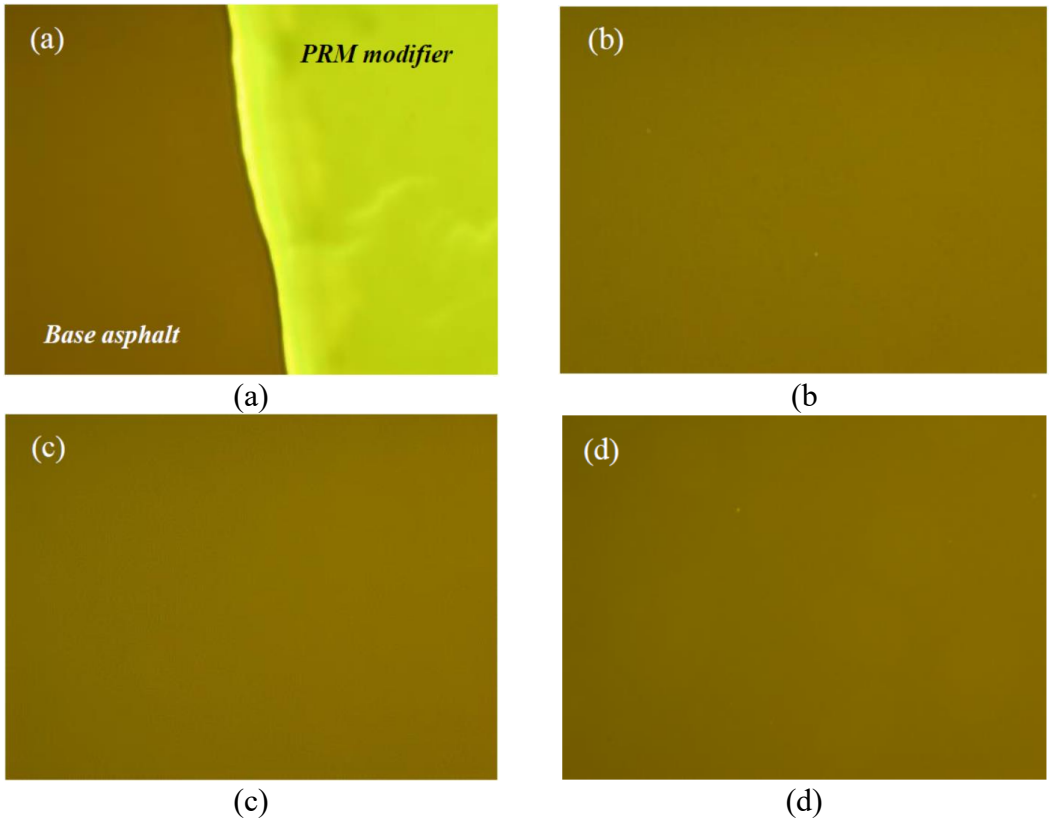

Fig. 14. FM micrographs at 19°C for the asphalt binders. (a) DS 70# base asphalt (b) DS+1.5%. (c) DS+2.5%. (c) DS+4%.

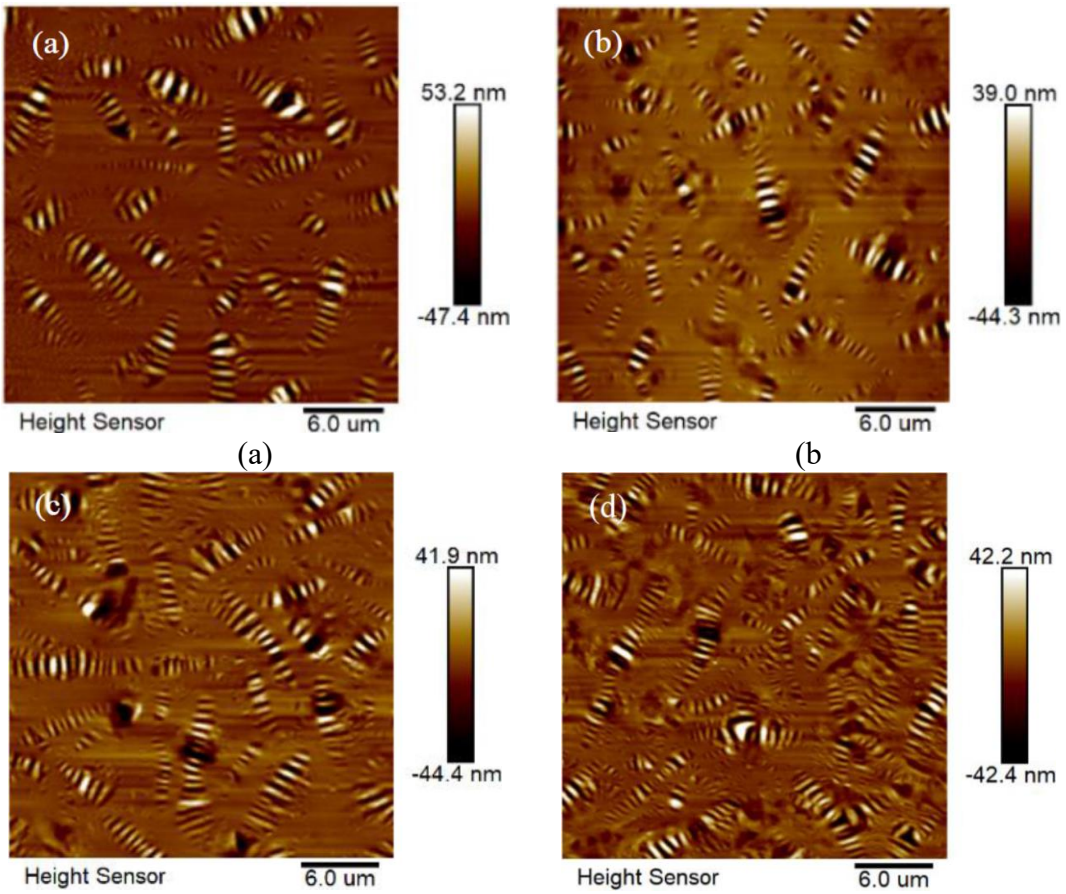

703 **Fig. 15.** AFM micrographs (30× 30 μm) at 20°C for the asphalt binders (a) DS 70#

704 base asphalt and. (b) DS+1.5%. (c) DS+2.5%. (d) DS+4%.